

# Energy Efficiency of a Multizone Office Building: MPC-based Control and Simscape Modelling

Farah Gabsi<sup>1</sup>, Frederic Hamelin<sup>1</sup>, Remi Pannequin<sup>1</sup> and Mohamed Chaabane<sup>2</sup>

<sup>1</sup>Centre de Recherche en Automatique de Nancy - University of Lorraine, Vandoeuvre-les-Nancy, France

<sup>2</sup>Laboratoire des Sciences et Techniques de l'Automatique et de l'informatique industrielle - ENIS, Sfax, Tunisia

**Keywords:** Energy-efficient Buildings, Simscape<sup>TM</sup> Models, Model Predictive Control, Multi-room Building Model.

**Abstract:** This paper deals with the problem of modelling and controlling a multi-zone office building to ensure its thermal comfort by an optimal and cost effective management of the energy consumption. A thermal behaviour analysis of the building is carried out using the Simscape<sup>TM</sup> library in MATLAB/Simulink<sup>®</sup> environment that leads to a multi-model representation. Based on this modelling, the Yalmip toolbox in the MATLAB programming environment or an iterative optimization algorithm can be used to solve the control optimisation problem. The design of a model predictive control associated with a wise choice of the cost function makes it possible to obtain in simulation substantial energy benefits.

## 1 INTRODUCTION

Over the last years, a large number of researchers have been interested in controlling strategies for energy saving of buildings (Scherer et al., 2014), (Atam and Helsen, 2016). Indeed, the construction sector, especially electrical energy, is the largest energy consumer. It represents approximately 40% of the total energy consumption between all sectors of the economy in France and in the US (Agbi, 2014). One of possible approaches to reduce energy consumption in buildings is to use advanced control tools to effectively monitor all the building actuators to ensure its hygrothermal comfort (Goyal et al., 2013), (Privara et al., 2011).

In this paper, a thorough methodology of modelling/controlling a building part is proposed to ensure the thermal comfort of its inhabitants while minimizing energy consumption. It uses the Simscape<sup>TM</sup> toolboxes to model the thermal behaviour of the building (Lapusan et al., 2016), and an iterative algorithm (or Yalmip (Lofberg, 2004)) to solve the optimization problem related to the synthesis of a predictive control. The applied target is the "Eco-safe" platform (CRAN Nancy, France) that fits in a global context of smart home. The developed Simscape<sup>TM</sup> model is based on a physical description of the building. This approach allows the description of the system as a physical structure rather than by abstract mathematical equations. Furthermore, the differential equa-

tions that describe the thermal behaviour of the system can be directly generated from the Simscape<sup>TM</sup> model. This modelling step in the form of a state-space representation is essential for the development of a predictive control model (MPC) (Camacho and Bordons, 2007). This type of control is favoured because it has the advantage of taking into account the disturbance predictions that greatly influence the interior comfort of a building (outside temperature, sunshine, occupations of parts) while anticipating their effects (Ma et al., 2011), (Oldewurtel et al., 2012), (Privara et al., 2011). Knowing that each control action is associated with a different state-space model of the system, the predictive control used is considered as a hybrid type (Le et al., 2014). In view of the control objectives, the associated optimization criterion is defined to integrate the energy cost of each actuator in *kWh*, the resolution of the optimization problem is executed using the Yalmip tool of Matlab or an iterative algorithm for important prediction horizon.

The first part of this work is focused on the thermal modelling of a set of building parts because few works have been interested in this issue. The validation of the model and the control will be conducted on the "Eco-safe" platform. Next a model predictive control is put in order to ensure the thermal comfort of the rooms of the platform with a minimum of energy consumption. Tests of simulation with various scenarios were developed to exhibit the energy benefits.

## 2 PLATFORM DESCRIPTION

The “Eco-safe” platform consists of 6 rooms and a corridor (Figure 1). The rooms are equipped with sensors and actuators to model their thermal behaviour and control their comfort. Regarding the area, the platform is characterized by two main activity rooms: “a room of research and development” (R&D, ①) of  $51m^2$  and a piece of applications ⑤ of  $34m^2$ . Four other rooms,  $17m^2$  each, allow to store tools and various materials (parts ②+④) or to have an estimate of the rooms temperature located in the upper and lower floors (③+⑥), because with the same neutral behaviour. The platform consists of heterogeneous equipment architecture such as the sensors needed for the modelling of its thermal response, the equipment contributing to the thermal comfort of the rooms and a weather station that integrates several sensors. To ensure the thermal comfort of this platform by implementing a predictive control based on the minimization of energy consumption, it is necessary to determine a model for the thermal behaviour of the platform. The following paragraph provides an answer to this objective through the definition of a simulator.

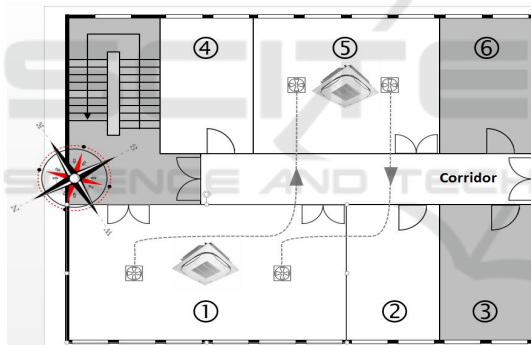


Figure 1: The “Eco-safe” deck plans.

## 3 THERMAL MODELLING OF THE PLATFORM

The simplified physical model we aim to establish has the role to predict the thermal behaviour of the whole platform. The latter is decomposed piece by piece taking into account their orientation in order to further simulate the influence of the solar radiation. Each room consists of different elements (walls, ceiling, floor, windows), some of which benefit from some solar energy inputs. The temperature of the R&D room, ① and applications ⑤ is also influenced by a main source of energy which is a reversible heat pump to produce the heat and cold. In addition, air flow is provided between these same rooms through

two controlled mechanical ventilation (CMV). Overall, the energy balance for each of the rooms can be translated by the following equation:

$$C_{int} \frac{dT_{int}}{dt} = f_{ext}(T_{ext}, T_{int}) + \sum_{i=1}^n f_i(T_{int}, T_{int,i}) + \theta_{occupancy} + \theta_{energy} \quad (1)$$

with:

- $C_{int}$ : heat capacity ( $J/K$ ) of the considered room;
- $T_{int}$ ,  $T_{ext}$  and  $T_{int,i}$ : temperature ( $K$ ) of the considered room, of outside and of the adjacent rooms;
- $\theta_{energy}$  and  $\theta_{occupancy}$ : energy contributions ( $W$ ) and heat generated by the inhabitants of the room;
- $f_{ext}(T_{ext}, T_{int})$  and  $f_i(T_{int}, T_{int,i})$ : functions reflecting the thermal behaviour of interfaces between the room and the outside or adjacent rooms.

In order to establish the complete thermal model of the “Eco-safe” platform, we use a physical approach based on the Simscape™ tool (Lapusan et al., 2016) in the environment Simulink®. The global model of the platform is the result of the integration of all room models. Each room includes walls and windows that are interacting with the external environment and neighbouring rooms by each mode of heat transfer. While this issue is the subject of the section that follows, the energy sources influencing the room thermodynamics are modelled in the last paragraph.

### 3.1 Thermal Modelling of a Room

The room model is developed using the thermal elements library of Simscape™. If a correspondence is established between the flow of heat and electric power as well as between the temperature and the potential difference, it is conventional to establish thermoelectric analogies (Achterbosch et al., 1985). This analogy will be used in the transcript of the Simscape™ model of the platform to a state-space model.

#### 3.1.1 Models of a Wall and a Set of Windows

**Wall:** The thermal equilibrium is established taking into account the convective exchange between the wall and the air that surrounds it on each side. Inside the wall, the heat is transferred through conduction phenomenon. The wall model developed on Simscape™ model is presented in Figure 2a, in which it is assumed that the wall is the interface between the inside of a room and the outside air. By electrical analogy, the wall can also be described by a 2R1C model (2 resistors and 1 capacitor) and schematically represented in Figure 2b, which presents the following notations:

- $X_1(p)$ ,  $X_2(p)$ ,  $T_{ext}(p)$ : temperature ( $K$ ) of the room, in the middle of the wall and of outside;
- $(R_{11}, R_{41})$  and  $(R_{21}, R_{31})$ : thermal resistances ( $K/W$ ) of convection and conduction;
- $C_{11}, C_{21}$ : heat thermal capacities ( $J/K$ ) of the room and of the exterior wall.

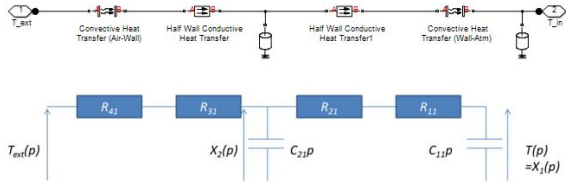


Figure 2: Model of a wall (a) by Simscape™ (b) by electrical analogy.

**Set of windows:** To model the thermal behaviour of all windows in a room, we assumed that it was identical to consider a single window of equivalent surface. Knowing that the windows in the rooms are all double glazed, their modelling requires to take into account not only the surface/superficial resistance of inside and outside exchange (transfer by convection/conductive transfer) but also transfers by conduction within the two glass panes and the air space between them (see Figure 3a). By analogy, a  $4R3C$  model is used to determine the associated state-space representation (see Figure 3b). with:

- $X'_1(p)$ ,  $X'_2(p)$ ,  $X'_3(p)$  and  $X'_4(p)$ : temperature ( $K$ ) of the room and in the middle of the inner glass, of the air space and of the outer glass;
- $(R_{12}, R_{82})$  and  $(R_{22}, R_{32}, \dots, R_{62}, R_{72})$ : thermal resistances ( $K/W$ ) of convection and conduction;
- $C_{22}, C_{32}, C_{42}$ : heat thermal capacities ( $J/K$ ) of the glass and of the air space/blade;

The state-space representations of a wall and of a set of windows are then obtained by the application of Millman's theorem.

### 3.1.2 Models of a Room and “Eco-safe” Platform

**Room:** A room being made up of several walls, a slab, a ceiling (whose thermal behaviour is similar to that of a wall in our case) and possible windows, the one-room model is obtained by the integration of the models of each of these elements within a unique state-space representation. Considering the R&D room (①) of the platform “Eco-safe” represented in Figure 4, the state-space model thus obtained is of order 11 (5 adjacent walls (order 1) + 1 ceiling (order 1) + 1 ground (order 1) + 1 set of windows (order 3) + heat capacity of the room (order 1)).

**“Eco-safe” Platform:** The platform is modelled by a set of rooms delimited by the walls that are in thermal contact with the outside environment and neighbouring rooms. Applying the same technique of modelling than for room ①, we get a state-space representation of order 72 to simulate the thermal behaviour of the platform. In this model, the temperature values of the upper and lower floors are considered to be identical to those of the reference rooms (③+⑥).

## 3.2 Modelling of Energy Sources

The most important elements that produce the heat or cold inside the building are the reversible heat pump, the ventilation system and sun radiation. These different equipments/contributions of energy are modelled in this paragraph to be integrated in the simulator. The model also takes into account the effect of the people inside the platform and that of different electrical appliances that generate heat.

### 3.2.1 CMV

The CMV is used to circulate the air between rooms ① and ⑤ (see Figure 1). It is assumed that the air taken in the ‘source’ room is replaced by the outside air through the openings at the level of the windows. On the other hand, air received by the ‘destination’ room replaces a part of its air that is equally displaced through the openings at the level of the windows. If we take the example that the air flows from room ⑤ to room ①, the energy flows generated by the CMV are at the level of the ‘source’ room:

$$\phi_{CMV1}(t) = \frac{\rho C_1 D_{CMV}}{3600} (T_{ext}(t) - T_{⑤}(t)) \quad (2)$$

and at the level of the ‘destination’ room:

$$\phi_{CMV2}(t) = \frac{\rho C_1 D_{CMV}}{3600} (T_{⑤}(t) - T_{①}(t)) \quad (3)$$

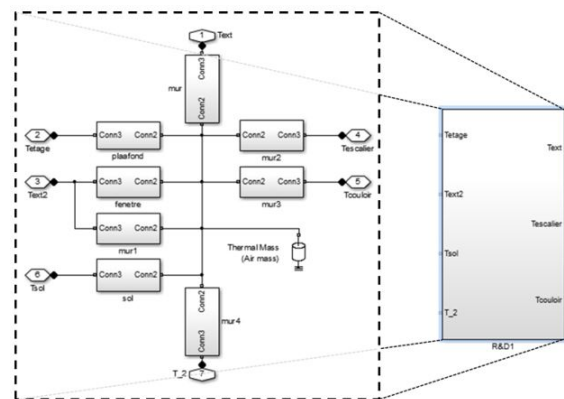


Figure 4: Model Simscape™ exhibit R&D (①).

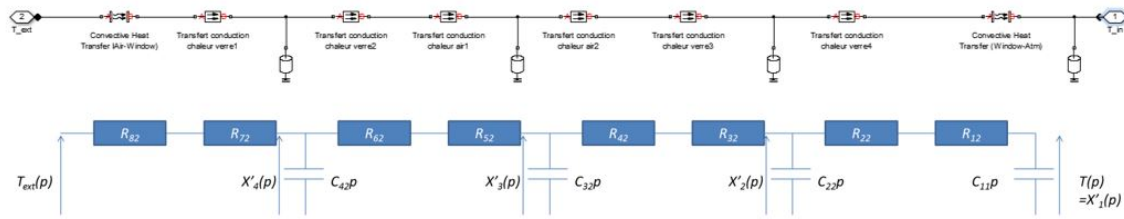


Figure 3: Model of a set of windows (a) by Simscape™ (b) par electrical analogy.

with  $c_1 = 1005.4 \text{ J/kg/K}$  the specific heat of air ;  $\rho = 1.204 \text{ kg/m}^3$  the density of air ;  $D_{CMV} = 150 \text{ m}^3/h$  the air flow of the CMV ;  $(T_{ext}, T_{\textcircled{1}}, T_{\textcircled{5}})$  the temperatures ( $K$ ) of outside atmosphere, of rooms  $\textcircled{1}$  and  $\textcircled{5}$ .

### 3.2.2 Reversible Heat Pump (HP)

A heat pump is a thermodynamic device that allows capturing heat from outdoor air and transmitting it inside the building. Being reversible, the HP air – water of the platform is capable of providing air conditioning in the summer. It starts running in heating mode in the order of  $312K$  and  $290K$  into cooling mode. Essentially, and without taking into account the transitional aspects, the equation translating this energy flow is in the heating mode:

$$\phi_{HP1}(t) = \frac{\rho c_1 D_{HP}}{3600} (312 - T_i(t)) \quad (4)$$

and in air conditioning mode:

$$\phi_{HP2}(t) = \frac{\rho c_1 D_{HP}}{3600} (290 - T_i(t)) \quad (5)$$

with  $D_{HP} = 5000 \text{ m}^3/h$  the air flow of the HP and  $T_i$  the room temperature ( $K$ ) in which the HP is used.

### 3.2.3 Modelling of the Occupation

Each individual has a sensible heat (by his/her body at  $37^\circ C$ ) and a latent heat (by his/her production of steam in breathing and perspiration). Different values are given in the literature (ASHRAE, 2013). A person generates about  $100W$ . By multiplying this value by the number of people in a room, we get the energy released by them.

### 3.2.4 Inputs of Energy by Solar Radiation

The sun provides heat that greatly influences the temperature within the platform rooms. The estimated brought solar energy requires to instantly follow the positioning of the sun and to take into account the radiation so that diffuse direct. In order to understand the calculations to quantify the global radiation, it is

important to define not only the various solar components, but also the different angles used for calculations (Antonic, 1998). The energy related to the direct radiation is such that:

$$S = 1230 \exp\left(-\frac{1}{3.8 \sin(h + 1.6)}\right) \cos(\beta) \quad (6)$$

where  $h$  is the height of the sun and  $\beta$  is the angle between the normal to the windows and the solar rays. They depend on the the latitude, the hour angle, the solar declination and the solar azimuth. As for the energy associated to the diffused radiation energy, it is calculated by the relationship :

$$D = 125(\sin(h)^{0.4})((1 + \cos(i))/2) + alb(((1 + \cos(i))/2)(1080(\sin(h)^{1.22}) - 125(\sin(h)^{0.4}))) \sin(h) + 125(\sin(h)^{0.4})(1 - \sin(h)) \quad (7)$$

where  $alb = 0.2$  is the albedo and  $i = 90$  corresponds to the inclination of the windows according to the horizontal.

## 3.3 Simulation Results

The simulator is implemented by integrating the set of energy sources described in the previous paragraph to the Simscape™ model of the ‘‘Eco-safe’’ platform. The associated state-space representation is determined by adding these different energy sources on the equivalent electrical schemas/diagrams in terms of the correspondence between a heat flow and an electric current. The use of the CMV or HP has the effect of changing the state-space model of the system. Considering different scenarios of following control, it is possible to define 6 state-space models of the platform:

- Scenario 0: no action on the system,
- Scenario 1: CMV switched room  $\textcircled{5}$  to  $\textcircled{1}$ ,
- Scenario 2: CMV switched room  $\textcircled{1}$  to  $\textcircled{5}$ ,
- Scenario 3: HP operated in the room  $\textcircled{1}$ ,
- Scenario 4: HP operated in the room  $\textcircled{5}$ ,
- Scenario 5: 2 HP operated in rooms  $\textcircled{1}$  and  $\textcircled{5}$ .

For simulation, continuous time models are finally discretized with a 5-min sampling period. They become:

$$\begin{cases} x(k+1) = A_i^{sim}x(k) + B_i^{sim}d(k) \\ y(k) = C^{sim}x(k) \end{cases} \quad (8)$$

with:

- $i \in \{0, \dots, 5\}$ : the type of implemented control on the system identically to the number of scenario;
- $A_i^{sim}$  and  $B_i^{sim}$ : state and input matrices associated with the number of scenario;  $C^{sim}$ : output matrix;
- $x(k) \in \mathbb{R}^{72}$ : state vector grouping all temperatures of walls, windows and rooms of the platform.
- $d(k) = [T_{ext,k} \ Occ_k \ Sol_{west,k} \ Sol_{east,k} \ T_{HP,k}]^T$ ;
- $y(k) = [T_{(1),k} \ T_{(2),k} \ T_{corridor,k} \ T_{(4),k} \ T_{(5),k}]^T$ ;
- $T_{ext,k}$ : outside temperature (K);
- $Occ_k$ : energy brought by occupants of room ①;
- $Sol_{west,k}$  and  $Sol_{east,k}$ : energy provided by solar radiation for rooms ①, ②, ③ and ④, ⑤, ⑥ resp.;
- $T_{HP,k}$ : temperature of the air forced through the HP,  $T_{HP,k}=290K$  (cold mode) or  $312K$  (hot mode).

Parameters  $R_{ij}$  and  $C_{ij}$  of the simulator were calculated from the nature and characteristics of the different materials used in the wall dividers, walls and windows of the platform. They have been adjusted from the temperature curves actually observed on the system. According to figures 7a and 7b, it appears that the profiles of actual and estimated temperature values are found to be very similar. The simulated curves were generated according to the different scenarios of control represented in Figure 6b and from the entries  $T_{ext,k}$  (Figure 5),  $Sol_{west,k}$  and  $Sol_{east,k}$  (Figure 6a), which are the data issued from the meteorology station over the period 14/09/2016 - 20/09/2016. Figure 8b represents the temperature estimated by the simulator within rooms ① and ⑤ in scenario 0. In addition to the previous inputs, the energy released from occupancy  $Occ_k$  (figure 8a) is also considered. The latter represents approximatively the energy generated by 24 people in room ① assuming their presence all the open days from 8h to 12h and from 14h to 18h.

The following paragraph aims to implement a control law on the platform, which is capable of ensuring thermal comfort in the occupied rooms while minimizing energy consumption. A predictive control is used on the basis of the simulator of the platform.

## 4 PREDICTIVE CONTROL

The principle of the predictive control (Camacho and Bordons, 2007) is to optimize a cost function allowing to describe the aim of control over a finite time

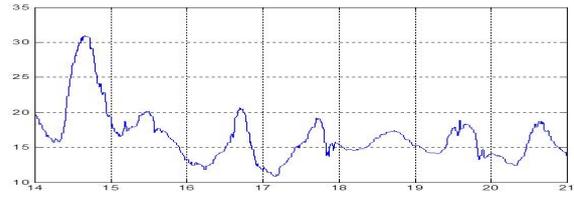


Figure 5: Outside temperature (14/09 - 20/09/2016).

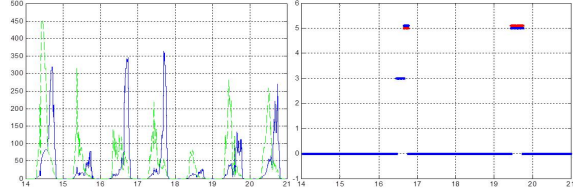


Figure 6: (a) Solar energy (W)  $Sol_{west,k}$  (green) and  $Sol_{east,k}$  (blue), (b) Control scenarios: HP in cold mode on 16/09 and hot mode on 19/09 in room ① (inversely for room ⑤).

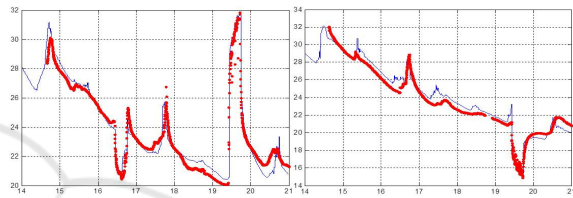


Figure 7: Actual (in red line) and estimated (in blue line) temperature values of (a) room ①, (b) room ⑤.

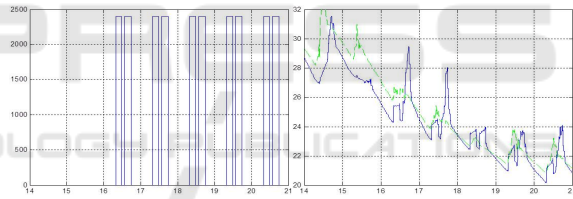


Figure 8: (a)  $Occ_k$ , (b) estimated temperature in rooms ① ( $T_{(1),k}$  in green) and ⑤ ( $T_{(5),k}$  in blue).

horizon. To calculate the sequence of controls that minimizes this cost function, we offer the platform ‘‘Eco-safe’’ a multi-model linear representation to predict its behaviour. At each moment, an optimal control sequence is calculated to minimize the cost function on a prediction horizon. Only the first element is applied to the system. As part of our application, this procedure is repeated every 5 minutes.

### 4.1 Cost Function and Constraints

Since the objective is to ensure the thermal comfort with a minimum of energy consumption, the cost function must reflect these performances in a mathematical formulation. In the light of the European thermal regulation ISO7730 and ASHRAE 55 standard, which define the thermal comfort as a temperature interval defined by a lower limit and an upper limit and according to the nature of the models of the

platform, the cost function is chosen such that:

$$J_1 = \min_{i_1, \dots, i_N} \sum_{j=1}^N \|y_{i_j}(k+j) - y_{ref}\|_Q^2 + cost(k+j) \quad (9)$$

where:

- $y_{min} \leq y_{i_j}(k+j) \leq y_{max}$  ;  $y_{ref} = \frac{y_{min} + y_{max}}{2}$
- $$\begin{cases} x'(k+1) = A_{i_j}^{com} x'(k) + B_{i_j}^{com} \hat{d}(k) \\ y_{i_j}(k) = C^{com} x'(k) \\ cost(k) = \alpha_{i_j} \end{cases}$$
- $\hat{d}(k) = [\widehat{T_{ext,k}} \quad \widehat{Occ_k} \quad \widehat{Sol_{west_k}} \quad \widehat{Sol_{east_k}} \quad \widehat{T_{HP,k}}]^T$  includes all the estimations of the disturbances.  $\widehat{T_{ext,k}}$ ,  $\widehat{Sol_{west_k}}$  and  $\widehat{Sol_{east_k}}$  are issued from meteorological forecasts in the short term ( $\widehat{Sol_{west_k}}$  and  $\widehat{Sol_{east_k}}$  require a basic calculation according to the orientation of the windows and predicted solar radiation).  $\widehat{Occ_k}$  is a prediction based on a planning of the energy generated by the people in the room
  - ①.  $\widehat{T_{HP,k}}$  depends on the value of  $i_j$  (see below).
- $i_j \in \{0, \dots, 8\}$  represents the used control scenario (cf. part 3.3) and  $\alpha_{i_j}$  the associated energy cost:
  - $i_j=0$ : Scenario 0,  $\alpha_0=0Wh$  and  $\widehat{T_{HP,k}}=0$ ,
  - $i_j=1$ : Scenario 1,  $\alpha_1=30Wh$  and  $\widehat{T_{HP,k}}=0$ ,
  - $i_j=2$ : Scenario 2,  $\alpha_2=30Wh$  and  $\widehat{T_{HP,k}}=0$ ,
  - $i_j=3$ : Scenario 3,  $\alpha_3=1000Wh$  and  $\widehat{T_{HP,k}}=290K$ ,
  - $i_j=4$ : Scenario 4,  $\alpha_4=1000Wh$  and  $\widehat{T_{HP,k}}=290K$ ,
  - $i_j=5$ : Scenario 5,  $\alpha_5=2000Wh$  and  $\widehat{T_{HP,k}}=290K$ ,
  - $i_j=6$ : Scenario 3,  $\alpha_6=1000Wh$  and  $\widehat{T_{HP,k}}=312K$ ,
  - $i_j=7$ : Scenario 4,  $\alpha_7=1000Wh$  and  $\widehat{T_{HP,k}}=312K$ ,
  - $i_j=8$ : Scenario 5,  $\alpha_8=2000Wh$  and  $\widehat{T_{HP,k}}=312K$ .
- Matrices  $A_i^{com}$ ,  $B_i^{com}$  and  $C^{com}$  are such that they define a reduced-order model of the simulator for  $0 \leq i \leq 5$ , whereas we have  $A_i^{com} = A_{i-3}^{com}$  and  $B_i^{com} = B_{i-3}^{com}$  for  $6 \leq i \leq 8$  considering that the energy consumption of HP in warm mode is exactly the same as in cool mode. Indeed, the order of the simulation system, being important (72), the calculations that would require the development of an optimal control would become very complicated and time consuming. Without immersing into the theoretical details of this model reduction, matrices  $A_i^{com}$ ,  $B_i^{com}$  and  $C^{com}$  are obtained through the determination of balanced state-space realizations. Furthermore, in order not to overly complicate the synthesis of the control law that normally requires the development of state observers to switch from one model to another, we have imposed on the systems of reduced order to be all of the order 5 (the number of temperature

sensors). This allows, for a simple basic change,  $C^{com} = I_5$  and initial state condition  $x'(0) = y(0)$ .

## 4.2 Optimization Problem

To minimize criterion  $J_1$ , the Yalmip software (in the Matlab environment) can be used (Lofberg, 2004). It turns out however that the design load increases with the horizon of prediction  $N$ . Also, due to the combinatorial explosion in computation time, for a number of control scenarios equal to 9 ( $i_j \in \{0, \dots, 8\}$ ), the value of  $N$  may not exceed 6. For larger values of  $N$ , using the Yalmip software no longer makes it possible to obtain a digital solution to the optimization problem. Yet, it can be very interesting to consider a more important prediction horizon. Indeed, a scenario of optimal control on a low prediction horizon may become inappropriate on a larger horizon. This happens especially when the heating and/or cooling capabilities of the building are modest or  $y_{min}$  and  $y_{max}$  are time-dependent. It is important to specify that temporal changes in  $y_{min}$  and  $y_{max}$  are beneficial in a context of minimization of the energy cost because the constraints in temperature of the parts of a building are not the same in the absence or in the presence of people.

Figures 9 and 10 illustrate this phenomenon in the simple case of a number of control scenarios equal to 4 and when  $y_{min}$  and  $y_{max}$  are time-dependent. Figure 9 shows in red the control scenario predicted from  $k+1$  until  $k+4$  (in agreement with the cost function  $J_1$  plotted vertically to the right of the figure) for  $y_{min}$  and  $y_{max}$  constant. It is characterized by the sequence of controls  $i_1 = 2$ ,  $i_2 = 3$ ,  $i_3 = 2$  and  $i_4 = 3$ . In the case of  $y_{min}$  and  $y_{max}$  become time-dependent (figure 10), it should be noted that the sequence of optimal controls becomes  $i_1 = 1$ ,  $i_2 = 2$ ,  $i_3 = 1$  and  $i_4 = 1$  (always in agreement with  $J_1$  plotted to the right of the figure). Therefore, in this example, if the prediction horizon  $N$  is chosen equal to 1, 2 or 3, the optimal control scenario to be applied at time  $k$  is associated to  $i_1 = 2$  whereas it is associated to  $i_1 = 1$  for  $N = 4$  and greater. In order to consider a prediction horizon up some hours, we will subsequently use an iterative approach. Its goal is to approach the best scenario of optimal control on a given prediction horizon while controlling the design load. The idea is to subdivide at iteration  $j$  interval  $I_j$  defined by:

$$I_j = [\max(y_{min}, \min_{i_j} \hat{y}_{i_j}(k+j) | \hat{y}(k+j-1)), \min(y_{max}, \max_{i_j} \hat{y}_{i_j}(k+j) | \hat{y}(k+j-1))] \quad (10)$$

in an ordered set of  $n$  small-intervals  $I_{j,l}$  with the same width:

$$I_j = \bigcup_l I_{j,l} \quad (11)$$

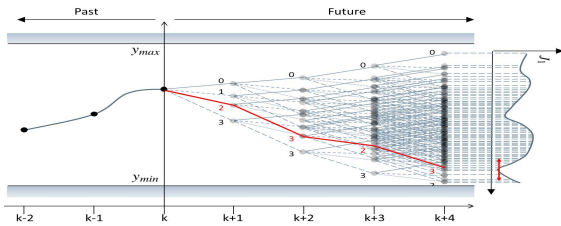


Figure 9: Control scenario predicted from  $k + 1$  until  $k + 4$  for  $y_{min}$  and  $y_{max}$  constant.

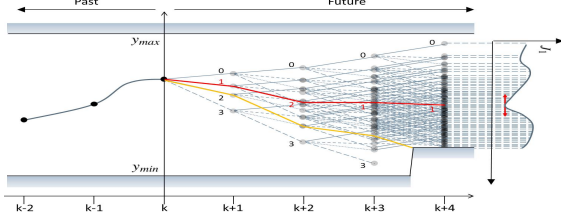


Figure 10: Control scenario predicted from  $k + 1$  until  $k + 4$  for time-dependent  $y_{min}$  and  $y_{max}$ .

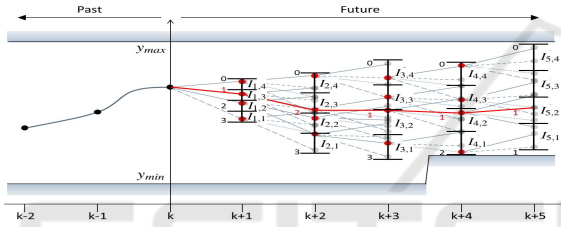


Figure 11: Control scenario predicted for time-dependent  $y_{min}$  and  $y_{max}$  using an iterative approach.

In this expression,  $\hat{y}(k) = y(k)$  and  $\hat{y}_{i_j}(k+j) | \hat{y}(k+j-1)$  represents  $n$  predictions of  $y$  at  $k+j$  from the model associated with control scenario  $i_j$  and from  $n$  particular predictions of  $y$  made the iteration before ( $j-1$ ). At each of the intervals  $I_{j,l}$  is joined a set of predictions  $\hat{y}_{i_\alpha}(k+j)$ . In order to remove the control scenarios associated to a more important energy cost than others, it keeps only a unique prediction  $\hat{y}(k+j)$  per interval  $I_{j,l}$ . It corresponds to the smallest value of  $\hat{y}_{i_\alpha}(k+j)$ . Figure 11 represents the principle of the proposed iterative approach on the same example as before with  $n = 4$ ,  $N = 5$ ,  $i_j \in \{0, \dots, 3\} = I$  and  $|I| = 4$ : number of members of  $I$ . At every moment of prediction, the  $n$  best predictions  $\hat{y}(k+j)$  (in the sense of cost function  $J_1$ ) are represented in red on the diagram. It can be observed that the scenario of optimal control  $i_1 = 1$ ,  $i_2 = 2$ ,  $i_3 = 1$  and  $i_4 = 1$  is the same as one obtained by considering all the control scenarios in a comprehensive way. On the other hand, the computational load is greatly reduced with the iterative algorithm. Indeed, if the number of calculations to predict  $\hat{y}(k+j)$  is of  $|I|(nN - n + 1)$  for this algorithm when  $\dim(y) = 1$ , it becomes maximum of  $(|I|^{N+1} - |I|)/(|I| - 1)$  by exhaustive research.

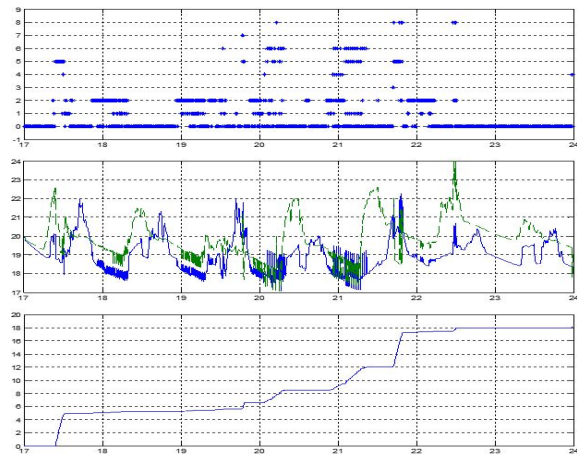


Figure 12: (a) Control scenarios, (b) temperature of rooms  $T_{\textcircled{1},k}$  (blue) and  $T_{\textcircled{5},k}$  (green), (c) kWh energy cost for  $Q = 0$  and  $N = 30$ .

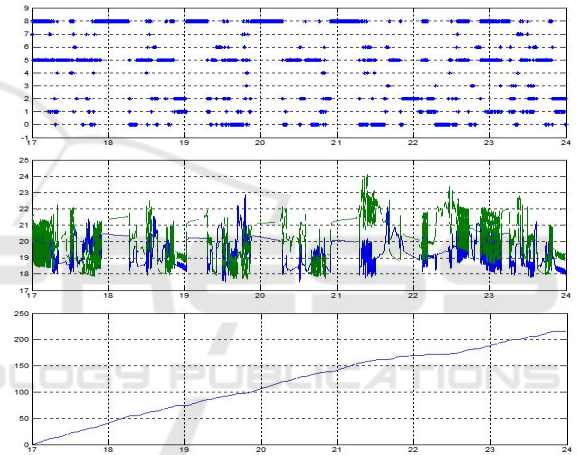


Figure 13: (a) Control scenarios, (b) Temperature of rooms  $T_{\textcircled{1},k}$  (blue) and  $T_{\textcircled{5},k}$  (green), (c) kWh energy cost for  $Q = \text{diag}([10^4 \ 0 \ 0 \ 0 \ 10^4])$  and  $N = 3$ .

### 4.3 Simulation tests

Aiming to illustrate the above approach and knowing that the main rooms of the platform are  $\textcircled{1}$  and  $\textcircled{5}$  rooms, the vectors  $y_{min}$  and  $y_{max}$  are chosen such that  $y_{min} = [18 \ 16 \ 16 \ 16 \ 18]$  and  $y_{max} = [23 \ 25 \ 25 \ 25 \ 23]$ . Figures 12 - 13 represent the evolution of temperatures  $T_{\textcircled{1},k}$  and  $T_{\textcircled{5},k}$  as well as the different scenarios of the control with their associated energy cost in kWh over the period 17/05 - 23/05/2016 for different values of  $N$  and  $Q$ . The inputs of the simulator are  $T_{ext,k}$  (Figure 14),  $Sol_{west,k}$  and  $Sol_{east,k}$  (figure 15b) and  $Occ_k$  (figure 15a). By these different simulations, the effect of the term  $\sum_{j=1}^N \|y_j(k+j) - y_{ref}\|_Q^2$  can be clearly seen on the optimal order scenario. The more  $\|Q\|$  is important, the more actuators with high power energy are so

licated (HP in our case) in on-off (hot-cold) control in order to maintain the temperature of the rooms ① and ⑤ close to  $y_{ref} = \frac{y_{min} + y_{max}}{2} = 20.5^{\circ}C$ . This type of scenario is highly energy-consuming (see Figure 13c compared to Figure 12c). Similarly, a low prediction horizon  $N$  makes the control more pre-emptive, resulting in a slight increase in the cost of energy in  $kWh$ .  $N$  equal to 30 samples (equivalent to 150 minutes) seems to be the best adapted in view of the ability of cooling/warming of the two HP.

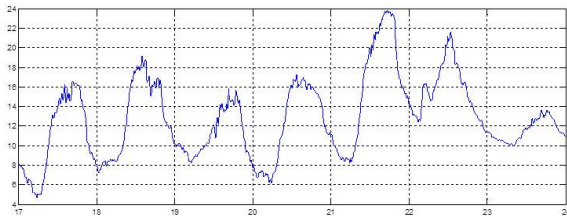


Figure 14: Outside temperature (17/05 - 23/05/2016).

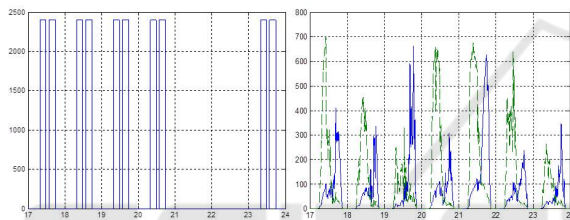


Figure 15: (a)  $Occ_k$ , (b) Solar energy (W)  $Sol_{west_k}$  (green) and  $Sol_{east_k}$  (blue).

## 5 CONCLUSION

In this paper, a whole simulator of the thermal behaviour of a building platform has been established. In a relatively high order (72), this simulator integrates the behaviours of the set of the partitions wall dividers/walls/windows of the platform rooms and all energy sources (solar radiation, temperature, rooms' occupancy, ventilation (CMV), heat pumps). Based on a multi model representation of the building and on an energy cost function in  $kWh$ , a predictive control has been successfully implemented to ensure the thermal comfort of the platform rooms with a minimum of energy consumption.

## ACKNOWLEDGEMENTS

This work was supported by the 7th Framework Programme FP7-NMP-608981 "Energy IN TIME" and has financial support from the Contrat de Plan Etat-Région (CPER) 2015-2020, project "Matériaux, Energie, Procédés".

## REFERENCES

- Achterbosch, G. G. J., Jong, P. P. G. D., Krist-Spit, C. E., Meulen, S. F. V. D., and Verberne, J. (1985). The development of a convenient thermal dynamic building model. *Energy and Buildings*, 8:183–196.
- Agbi, C. (2014). *Scalable and Robust Designs of Model-Based Control Strategies for Energy-Efficient Buildings*. Dissertations, Carnegie Mellon University - <http://repository.cmu.edu/dissertations/333>.
- Antonic, O. (1998). Modelling daily topographic solar radiation without site-specific hourly radiation data. *Ecological modelling*, 113(1-3):31–40.
- ASHRAE (2013). *ASHRAE Handbook - Fundamentals (SI Edition)*. American Society of Heating, Refrigerating and Air-Conditioning Engineers, Inc.
- Atam, E. and Helsen, L. (2016). Control-oriented thermal modeling of multizone buildings: Methods and issues: Intelligent control of a building system. *IEEE Control Systems*, 36(3):86–111.
- Camacho, E. F. and Bordons, C. (2007). *Model predictive control*. Advanced textbooks in control and signal processing. Springer-Verlag London.
- Goyal, S., Ingley, H. A., and Barooah, P. (2013). Occupancy-based zone-climate control for energy-efficient buildings: Complexity vs. performance. *Applied Energy*, 106:209–221.
- Lapusan, C., Balan, R., Hancu, O., and Plesa, A. (2016). Development of a multi-room building thermodynamic model using simscape library. *Energy Procedia*, 85:320–328.
- Le, K., Bourdais, R., and Gueguen, H. (2014). Optimal control of shading system using hybrid model predictive control. In *2014 European Control Conference (ECC)*, pages 134–139, Strasbourg, France.
- Lofberg, J. (2004). Yalmip: a toolbox for modeling and optimization in matlab. In *2004 IEEE International Symposium on Computer Aided Control Systems Design (CACSD)*, pages 284–289, Taipei, Taiwan.
- Ma, Y., Borrelli, F., Hency, B., Coffey, B., Bengesa, S., and Haves, P. (2011). Model predictive control for the operation of building cooling systems. *IEEE Transactions on Control Systems Technology*, 20(3):796–803.
- Oldewurtel, F., Parisio, A., Jones, C. N., Gyalistras, D., Gwerder, M., Stauch, V., Lehmann, B., and Morari, M. (2012). Use of model predictive control and weather forecasts for energy efficient building climate control. *Energy and Buildings*, 45:15–27.
- Privara, S., Siroky, J., Ferkl, L., and Cigler, J. (2011). Model predictive control of a building heating system: The first experience. *Energy and Buildings*, 43(2-3):564–572.
- Scherer, H., Pasamontes, M., Guzman, J., Alvarez, J., Camponogara, E., and Normey-Rico, J. (2014). Efficient building energy management using distributed model predictive control. *Journal of Process Control*, 24(6):740–749.